IEEE Access
Multidisciplinary | Rapid Review | Open Access Journal

Received March 30, 2019, accepted May 13, 2019, date of publication June 10, 2019, date of current version June 25, 2019.

*Digital Object Identifier 10.1109/ACCESS.2019.2921813*

# Application of Chaos Synchronization Technique and Pattern Clustering for Diagnosis Analysis of Partial Discharge in Power Cables

**FENG-CHANG GU, HER-TERNG YAU, AND HUNG-CHENG CHEN**
Department of Electrical Engineering, National Chin-Yi University of Technology, Taichung 41107, Taiwan

Corresponding author: Hung-Cheng Chen (hcchen@ncut.edu.tw)

This work was supported by the National Science Council of the Republic of China under Grant MOST 107-2221-E-167-015 and Grant MOST 107-2218-E-167-002-MY2.

**ABSTRACT** This paper primarily discusses the measurement of partial discharge (PD) phenomena and clustering in the defect pattern of a cross-linked polyethylene power cable joint. First, a high-speed data acquisition and pretreatment were performed for PD electrical signals at a sampling rate of 20 MS/s. The crucial characteristic signals were reversed to reduce the calculated amount of noise. A characteristic matrix was created according to the resulting dynamic error of chaos synchronization. The characteristic parameters were extracted using the fractal theory. Finally, the extension theory was used to develop a diagnostic system and anti-interference test. A comparison with the existing Hilbert–Huang transform (HHT) method revealed that the two characteristics extracted from the chaos synchronization results using the fractal theory were recognized at a higher pattern recognition rate by employing the extension theory. The proposed method can extract crucial information concerning PD as a defect in power cable joints.

**INDEX TERMS** Chaos synchronization, extension, fractal, Hilbert–Huang transform, partial discharge.

## I. INTRODUCTION

Power equipment comprises electrically conducting, magnetically conducting, and insulating materials. Insulating materials are critical for maintaining the quality of the power supply mechanism. If the equipment is always in a hostile environment or has been used for many years, then the equipment's insulation will deteriorate. Human error in the construction process or failure to meet working standards can destroy the insulation in equipment. According to statistics in the literature, most accidents that occur during the use of power equipment are caused by the deterioration of insulating materials or faults [1]–[4]. Various industrial systems other than power equipment also exhibit fault clustering, and the clustering of such faults has been closely investigated in recent years. Accurate clustering of fault type can improve the accuracy of fault diagnosis in industrial systems [5], [6].

The literature [7], [8] reveals that the universal characteristics of the partial discharge of power equipment include partial discharge phase, mean number of discharges, mean discharge, and discharge frequency. Common methods for analyzing frequency are the Fourier transform, discrete Fourier transform, and Hilbert–Huang transform [9], [10]. These are typically used to analyze defects in power equipment. Although these methods can directly capture characteristics from partial discharge signals, a large database is required to analyze the partial discharge characteristics, and determining long-term partial discharge characteristics is complex and time consuming. Moreover, fault types are not always completely classified. Partial discharge has been identified from the characteristics of the partial discharge signals on an elliptical locus. With advancements in science and technology, commercial partial discharge detectors are now capable of accurately measuring partial discharge phenomena [11]–[13]. These detectors identify partial discharge signals originating from the insulation of power equipment and analyze the partial discharge characteristics and gradual dielectric breakdown to provide equipment maintenance–related information to prevent severe accidents. However, the required commercial instruments generally cost between US$20,000 and US$50,000, and most of the detection instruments capture signals that have been pretreated by the

The associate editor coordinating the review of this manuscript and approving it for publication was Di He.

front-end circuit; thus, the analyzed partial discharge signals would lose some of their physical significance. Therefore, the aim of this study was to analyze and automatically identify signals measured using basic sensors.

Chaos is a peculiar characteristic of nonlinear systems in which a deterministic mathematical system exhibits random-like dynamic behavior. Chaos has been extensively studied in many engineering applications [14], [15], including adaptive control systems, signal processing, fluid mechanics, and communication secrecy. Its characteristics are high sensitivity to the initial value, fractal dimensionality, pseudo-randomness,, and unpredictability. This study analyzed partial discharge signals by applying the chaos synchronization concept. Appropriate parameters were used to enable the slave system to track the master system automatically, and the error dynamic between normal and defect signals were extracted [16]. Additionally, original defective signals were pretreated in the present study to extract characteristics effectively, reduce the computing time, reduce the amount of noise, and reverse the partial discharge characteristics.

This study was also conducted to diagnose defects in the insulation in a power cable and discuss latent insulation faults. Artificially defective power cables were measured. The defects were evaluated using four power cable models: a scratched insulating layer, an outer semi-conductive layer that exceeds the standard length, an outer semi-conductive layer that is much shorter than the standard length, and a healthy power cable. Commercial high-frequency current transformers were used to measure the partial discharge signals in the power cable at a sampling rate of 20 MS/s. Different defective power cables typically yield differently formed partial discharges. The position and partial discharge can be determined by the fact that the basic reference voltage (60 Hz) phase has different characteristics. In this study, the duration of one cycle (60 Hz) of the defect signals was considered the data sample period. In an ideal normal signal state, the defect signal has zero amplitude. The defect signals and normal signals were input into a master–slave chaos synchronization system in this study. The master–slave system tracked the differences between the trajectories of the defect signals and normal signals as characteristics. The same defect partial discharge was self-similar; therefore, each difference between trajectories was not considerable and exhibited unique characteristics. A characteristic matrix was determined from the difference between trajectories, and fractal theory was used to extract two crucial characteristics: fractal dimension and lacunarity [17]–[19]. Pattern recognition based on extension theory was applied to select the first 20 data points of various defects for training, and the remaining 20 data were used in testing. Comparing this scheme with the HHT method verified that the proposed clustering method uses fewer characteristics for clustering and can identify defects effectively. Chaos synchronization–based characteristic extraction is proven to be capable of obtaining crucial information from various defect signals.

## II. ERROR DYNAMICS OF CHAOS SYSTEMS

The partial discharge characteristics of power cables are transient in nature. Consequently, recording and analyzing these characteristics in real time poses a considerable challenge to conventional clustering methods based on large databases of historical data. Accordingly, the present study modeled the power cable as a master–slave chaos system in which the slave is controlled such that the master can be tracked within a cycle period. For master–slave systems, even small perturbations in the states of the master or slave have considerable effects on the chaotic behavior of the system. For example, loading different initial values into the chaotic system may result in completely different chaos phenomena, thereby leading to substantial changes in the magnitude and dynamics of the error signal. The present study exploited this ''small-signal'' characteristic to detect changes in the partial discharge (PD) state of the power cable such that the quality of the cable can be rapidly and reliably detected during its fabrication or subsequent service life.

In 2004, Chen and Lee proposed a new chaotic system [20] called the Chen–Lee system. It comprises the following system of nonlinear differential equations:

$$\begin{aligned}\frac{dx}{dt} &= -yz + ax \\ \frac{dy}{dt} &= xz + by \\ \frac{dz}{dt} &= \left(\frac{1}{3}\right)xy + cz\end{aligned} \tag{1}$$

where $x$, $y$, and $z$ are state variables and $a$, $b$, and $c$ are system parameters. The Chen–Lee chaos synchronization (CS) system has the following construction:

$$Master\ System: \begin{cases} \dfrac{dx_1}{dt} = ax_1 - y_1z_1 \\ \dfrac{dy_1}{dt} = by_1 + x_1z_1 \\ \dfrac{dz_1}{dt} = cz_1 + \frac{1}{3}x_1y_1 \end{cases} \tag{2}$$

$$Slave\ System: \begin{cases} \dfrac{dx_2}{dt} = ax_2 - y_2z_2 \\ \dfrac{dy_2}{dt} = by_2 + x_2z_2 \\ \dfrac{dz_2}{dt} = cz_2 + \frac{1}{3}y_1y_2 \end{cases} \tag{3}$$

If is the sampled data sequence of defect signals, and $y$ is the sampled data sequence of normal signals, then let the variables in Eq. (2) be $x_1 = x\ [i]$, $y_1 = x\ [i+1]$, $z_1 = x\ [i+2]$, and $x_2 = y\ [i]$, $y_2 = y\ [i+1]$, $z_2 = y\ [i+2]$, $i = 1, 2, \ldots, n-2$, where $n$ denotes the total number of sampled data in the complete cycle. Then the error states can be expressed as $e_1 = x_1\text{-}x_2$, $e_2 = y_1\text{-}y_2$, $e_3 = z_1\text{-}z_2$, and the error dynamic system (ED) can be obtained from

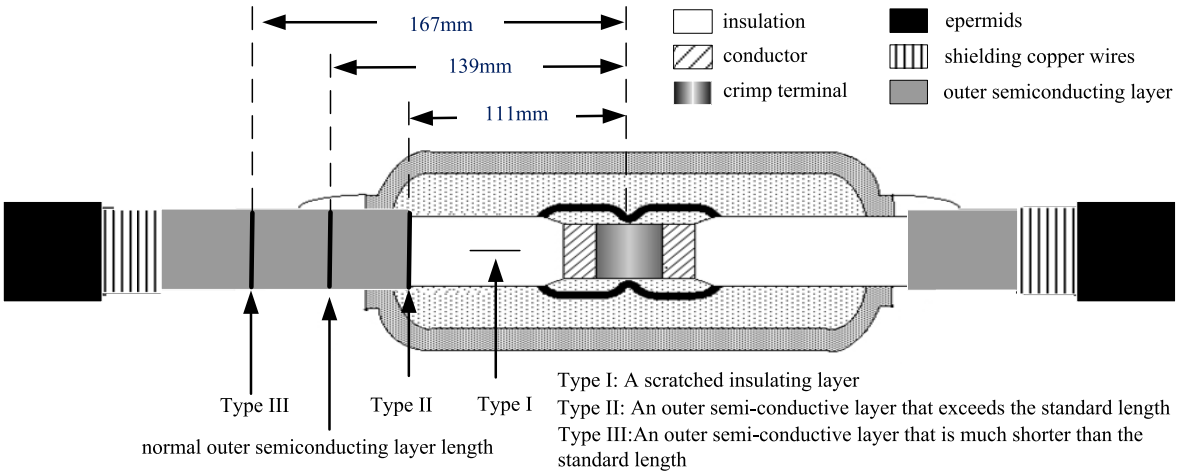


**FIGURE 1.** Defect models in power cable joint.

Eqs. (2) and (3):

$$\begin{cases} \dfrac{de_1}{dt} = E_1 = ae_1 - e_2e_3 - y_2e_3 - z_2e_2 \\ \dfrac{de_2}{dt} = E_2 = be_2 + e_1e_3 + z_2e_3 + x_2e_1 \\ \dfrac{de_3}{dt} = E_3 = ce_3 + \frac{1}{3}\left[e_1e_2 + x_2e_2 + y_2e_1\right] \end{cases} \tag{4}$$

In Eqs. (2) and (3), $a$, $b$ and $c$ are nonzero parameters. According to the literature [20], the system parameters $a$, $b$ and $c$ must satisfy $a > 0, b < 0, c < 0$, and $0 < a < -(b+c)$, and herein the Chen-Lee system has a chaotic attractor. The system parameters are selected as a = 3, b = −3, and c = −1. Then, the master-slave Chen-Lee chaotic system's dynamic trajectories move within a bounded range under different initial conditions.

## III. PD MEASUREMENT ENVIRONMENT SYSTEM

### A. DEFECT MODELS

Statistics in the literature indicate a high prevalence of cross-linked polyethylene (XLPE) power cable breakdowns in cable joints [21]. The specimens in this study were 25-kV XLPE power cable joints. Figure 1 shows defect models that may be caused by humans during power cable joint construction. This study simulated an insulation defect caused by a knife used by a worker to peel the insulation shield. The defect depth and length in the insulation were 2 and 20 mm, respectively, defined as a scratched insulating layer (Type I). In our measurement, the normal length of the cut made from the insulation shield to the conductor terminal should be 139 mm, with ±10% being an acceptable error range. We simulated an insulation shield cut of only 111 mm, which was 20% less than the normal length, defined as the case in which the outer semi-conductive layer exceeded the standard length (Type II). We simulated another cut of 167 mm, which was 20% more than the normal length, defined as the case in which the outer semi-conductive layer was shorter than the standard length (Type III). Finally, a non-defective power cable joint was also simulated (Type IV).

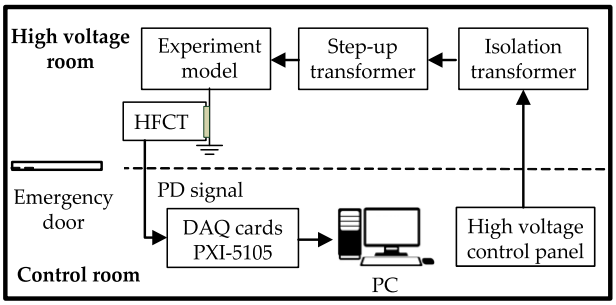


**FIGURE 2.** Block diagram of partial discharge detection system.

### B. MEASUREMENT ENVIRONMENT

In this investigation, measurements were made in a hyperbaric chamber that was divided into two parts in a control room. Figure 2 presents a block diagram of the partial discharge detection system. The signal detected in the control room, using a high voltage control panel for controlling the isolation transformer. The isolation transformer voltage is boosted, and then the high voltage side of a step-up transformer is connected to the conductor layer of the power cable. The ground and covering of the copper are connected to each other. The cable shielding current on the copper signal is measured using a commercial HFCT. The bandwidth of HFCT is between 500 kHz and 20 MHz. Figure 3 presents the shielding room and indoor cable used for the actual measurement. Finally, measurements were conducted under a condition involving a sampling rate of 20 MS/s and signal transmission to a NI PXI-5105 computer data acquisition card. Data were compiled using LABVIEW software for measurements at the man–machine interface of these partial discharge signals in real-time detection and storage. In the voltage step-up procedure of the PD measurement process,

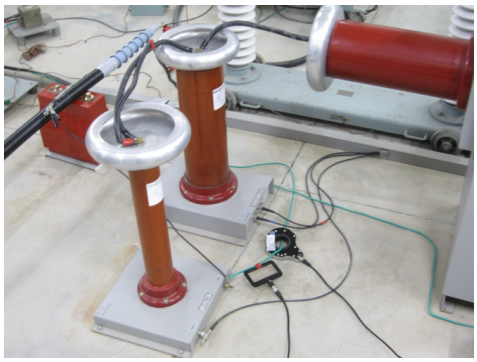

**FIGURE 3.** Measurement of a high-voltage power cable.

a 25-kV cable should have a 14.4-kV ($U_0$) rated phase-to-ground voltage. However, according to IEC 60502-2, for a power cable from 6 to 30 kV, the test voltage after installation should be 1.7 $U_0$ for 5 min [22]. Because the voltage must exceed the partial discharge inception voltage to excite the PD phenomenon, the test voltage should be $1.7 \times 14.4$ kV = 24.5 kV. Thus, 25 kV was selected as the test voltage. The high-voltage generator generated a rising voltage from 0 V to 25 kV. The HFCT then measured the power cable joint and recorded the signals after 1 min.

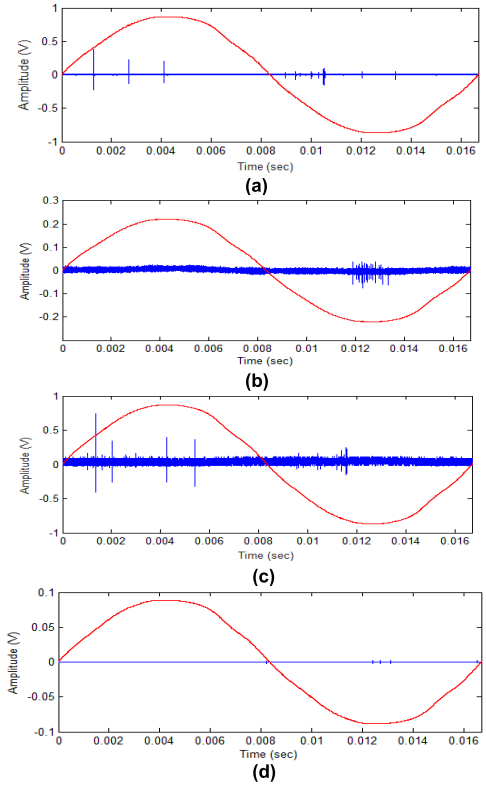


**FIGURE 4.** Electrical signal for different defect models of power cable. (a) Type I, (b) Type II, (c) Type III, and (d) Type IV.

Figure 4 shows the HFCT electrical signals in one cycle at 60 Hz for different specimens. The x-axis represents time in seconds, and the y-axis represents the signal amplitude (V).

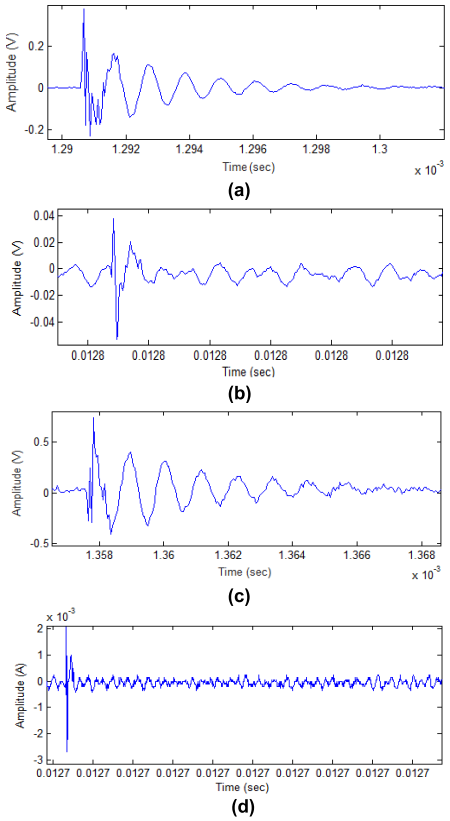


**FIGURE 5.** Typically single partial discharge signal for defect models. (a) Type I, (b) Type II, (c) Type III, and (d) Type IV.

Type I was observed to appear in both the positive and negative regions, with the corresponding voltage magnitude being approximately 0.35 V. Type II, representing the defect type with the highest number of discharges, occurred only in the negative region, with the corresponding voltage magnitude being only 60 mV. Type III discharge occurred in both the positive and negative regions, and the signal in the positive region was stronger than that in the negative region. The maximum amplitude was 0.7 V, which was higher than that in the other defect models. Type IV was considered the healthy power cable joint; its only noise was background noise, which was less than 5 mV and had no obvious signal. Figure 5 illustrates one PD pulse in the four defect models for a chaos synchronization system, as described by Eq. (4). A partial discharge event for each defect model can be characterized by such values as signal frequency and amplitude. Type IV was considered to belong to a healthy power cable joint; therefore, the measured signal was only a background signal.

### C. SIGNAL ANALYSIS METHOD

As in the study of Chen *et al.* [16], the present study considered four types of power cables. A total of 200 sampled data sequences were used for signal analysis. During the analysis, the master system (with defect signals) was considered the host system. The number of defect data in the range of 1–198 was denoted by $x_1$, the number of defect data

in the range of 2–199 was denoted by $y_1$, and the number of defect data in the range 3–200 was denoted by $z_1$. The slave system (with normal signals) was considered the chase reference system; the number of normal data in the range of 1–198 was denoted by $x_2$, the number of normal data in the range of 2–199 was denoted by $y_2$, and the number of normal data in the range of 3–200 was denoted by $z_2$. Through the execution of a subtraction process using Eqs. (2) and (3), this study determined the error dynamics $E_1$, $E_2$, and $E_3$ of the chase trajectory by using Eq. (4).

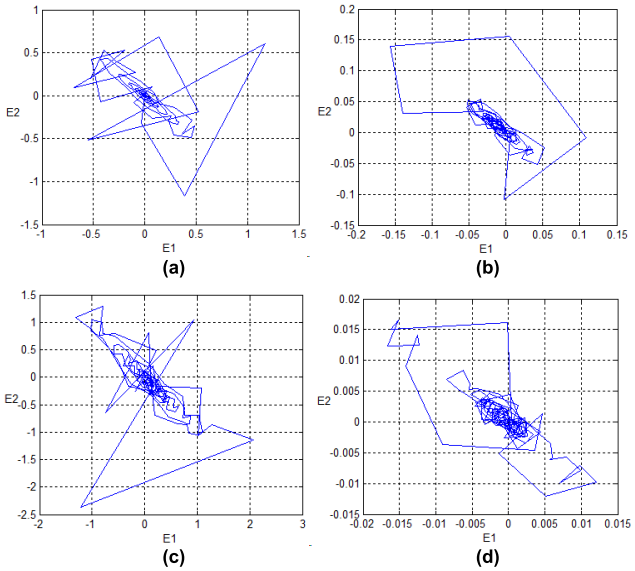


**FIGURE 6.** $E_1$, $E_2$ trajectory diagram of four defect types; (a) Type I, (b) Type II, (c) Type III, and (d) Type IV.

As revealed by the $E_1$, $E_2$ trajectory diagram in Figure 6, the trajectories of the various types of cables had clearly different shapes, paths, and sizes. Notably, however, each of the trajectories was self-similar. In addition, the different cable types had different bitmap distributions and densities, as presented in Figure 7. Thus, both the density between points and the number of distributed points can serve as useful indicators of cable type.

This study calculated three-dimensional (3D) characteristic graphs of the cables by applying fractal theory. Moreover, two characteristic values of each cable, namely the lacunarity and fractal dimension, were extracted from the characteristic matrix [15] using the CS and HHT methods. The characteristic values were then used to identify the cable type by executing a clustering algorithm based on extension theory.

Figure 8 presents the CS-derived 3D characteristics of the four cables. Notably, the distributions in Figure 8(a) and (c) are clearly different from those in Figure 8(b) and (d). Specifically, the characteristic distributions inFigure 8(a) and (c) are wider and the $\Sigma E_3$ value is higher compared with those in Figure 8(b) and (c). Figure 9 displays the HHT-derived 3D characteristics of the four cables [9], [10], [23].

The 3D n–q–$\varphi$ PD patterns that were transferred from the measured PD signals are presented in Figure 10. For the 3D

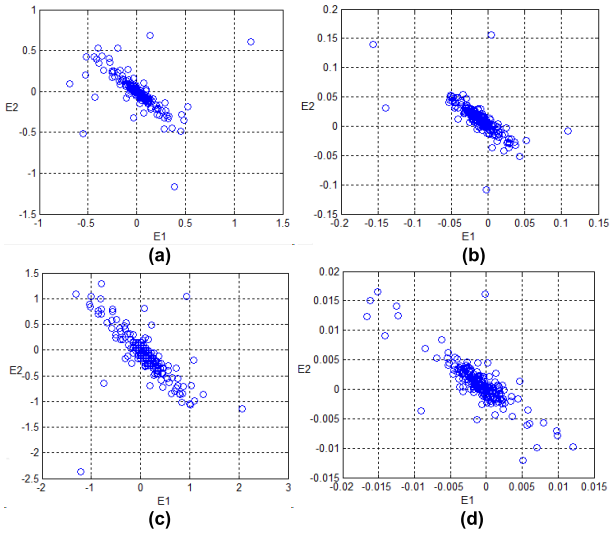


**FIGURE 7.** $E_1$, $E_2$ bitmap of four defect types; (a) Type I, (b) Type II, (c) Type III, and (d) Type IV.

n–q–$\varphi$ patterns, the primary parameters were the discharge magnitude ($q$), discharge number ($n$), and phase angle ($\varphi$). Types I and III exhibited higher discharge amplitudes in both the positive and negative periods compared with the other types. The maximum discharge was 225 pC, which belonged to Type III. Only in the negative period was discharge observed for Type II and IV. Type II had a maximum discharge of 37 pC. For Type IV, the equipment was virtually undamaged, and a relatively low amplitude of less than 10 pC was noted. As confirmed through experimentation, the extension theory–based pattern recognition technique proposed in this study could accurately differentiate types of defects.

## IV. RESULTS AND DISSCUSSION

### A. FEATURES EXTRACTION

A total of 160 partial discharge data points were obtained: 40 for each type of power cable. For each defect type, 20 data points were selected randomly for training, and the remaining 20 data points were used for testing. The chaos synchronization system developed in this study revealed the error dynamic trajectories $E_1$, $E_2$, and $E_3$, and a characteristic matrix was constructed using the error dynamic trajectory. The lacunarity and fractal dimension were determined using fractal theory. To elucidate the advantages of this method, a 3D characteristic matrix was established through HHT under the same conditions for comparison. Finally, the accuracy of the analysis that was performed using this scheme and HHT and the noise tolerance were evaluated with reference to the clustering results according to extension theory.

When the defects were analyzed through the CS and HHT methods, the lacunarity and fractal dimension were obtained using fractal theory. Figures 11 and 12 present the results. Each defect type had its own characteristic range. On the basis of the 3D characteristics of the various defect types in Figure 8, Type I and Type III defects were predicted to yield similar results and to have a larger fractal dimension

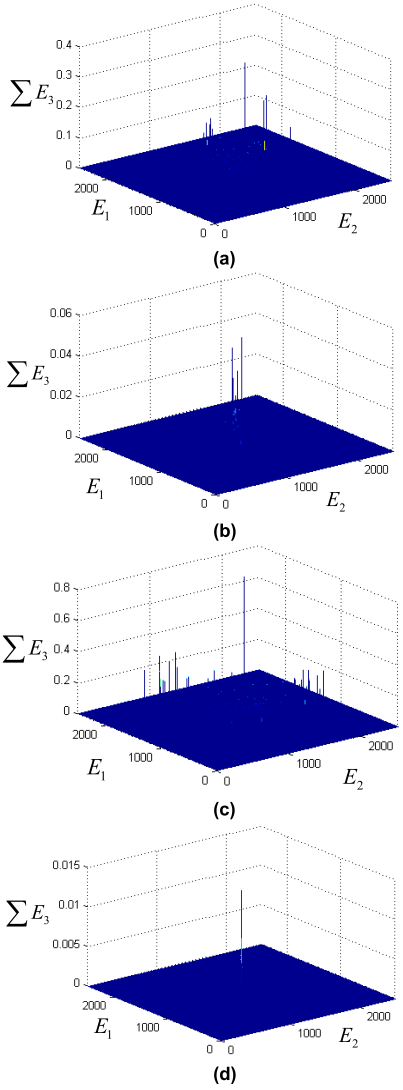


**FIGURE 8.** Three-dimensional characteristics of four defect models characterized by CS; (a) Type I, (b) Type II, (c) Type III, and (d) Type IV.

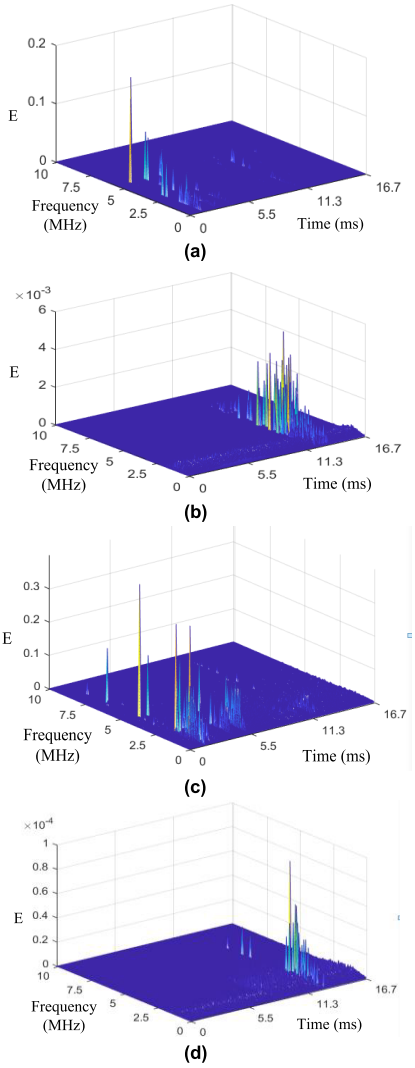


**FIGURE 9.** Three-dimensional characteristics of four defect models characterized by HHT; (a) Type I, (b) Type II, (c) Type III, and (d) Type IV.

than did Type II and Type IV defects. Because the total value of $E_3$ for Type I and Type III defects was higher than that for the other types, the fractal dimension was also larger. Figure 13 illustrates the fractal dimension distribution. The fractal dimensions for Type I and Type III defects were noticeably larger than those for the other two defect types. However, identifying variations among the four types with respect to only the fractal dimension was difficult. Therefore, the lacunarity of the various defect types was calculated. Figures 13 and 14 map the CS- and HHT-derived characteristics; as revealed in the figures, the HHT-derived characteristics could not clearly highlight the various defect types.

### B. RECOGNITION METHOD

Extension theory includes the concepts of matter element analysis and extension sets, and its main application is in solving contradiction and incompatibility problems [24]. Matter element analysis can easily represent the nature of matter, and the extension set is the quantitative tool of extension theory, which represents the correlation degree of the matter element according to the designed correlation function. The membership function of a traditional fuzzy set describes the value of matter in the interval [0, 1]. The extension set extends the fuzzy set from [0, 1] to $[-\infty, \infty]$. Consequently, it enables the definition of a set that includes any data in a particular domain [24], [25]. The proposed extension-based recognition method is described as follows.

**Step 1**: Formulate the matter-element $R_i$ for each defect type as

$$R_i = (T_i, C_j, V_j) = \begin{Bmatrix} T_i & c_1 & \langle a_{i1}, b_{i1} \rangle \\ & c_2 & \langle a_{i2}, b_{i2} \rangle \end{Bmatrix} \tag{5}$$

where

$T_i$: $i$th defect type of the PD pattern;

$C_j$: $j$th input feature;

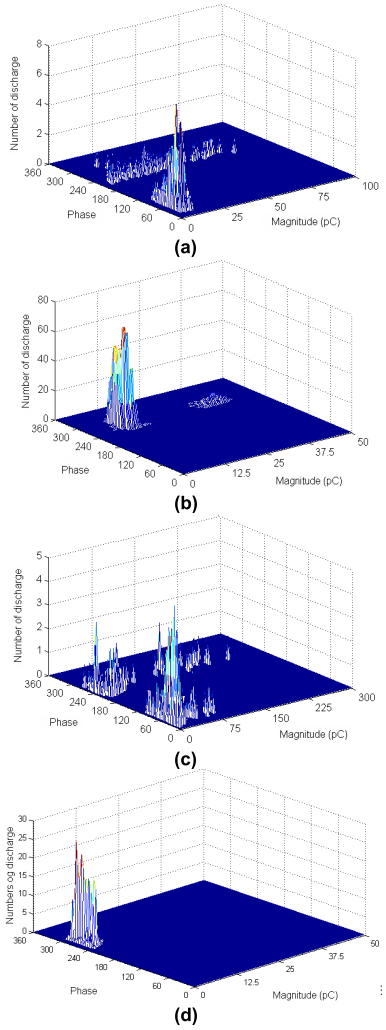


**FIGURE 10.** Four typical n-q-$\varphi$ PD patterns of experiment models. (a) Type I, (b) Type II, (c) Type III, and (d) Type IV.

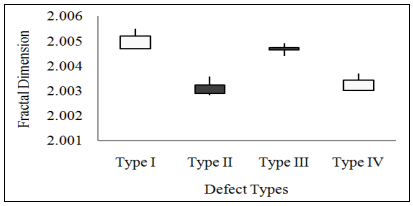


**FIGURE 11.** Distribution of the fractal dimension of four defects featured by CS.

$a_{ij}$: lower bound of classical domains related to the $j$th input feature of the $i$th defect type;

$b_{ij}$: upper bound of classical domains related to the $j$th input feature of the $i$th defect type.

The classical domain $V =< a, b >$ of each value falls between the lower and upper bounds on PD records. The neighborhood domain $\hat{V} = < f, g >$ of classical domains, which constitutes the possible range of each characteristic, can then be determined by setting $f = (1 - \alpha) \times a$ and $g = (1 + \alpha) \times b$, where $\alpha$ represents an extend factor [24]. The extension correlation function concept is presented in Figure 15.

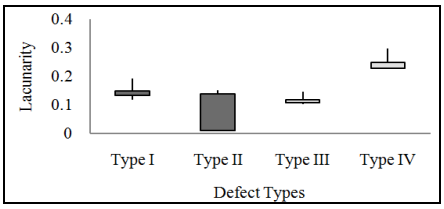


**FIGURE 12.** Distribution of the lacunarity of four defects derived by CS.

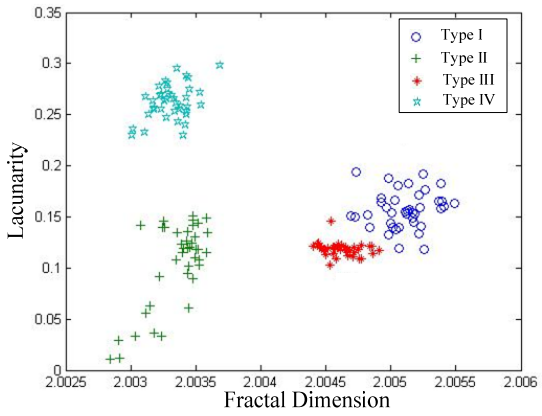


**FIGURE 13.** Characteristic distribution of four defects featured by CS.

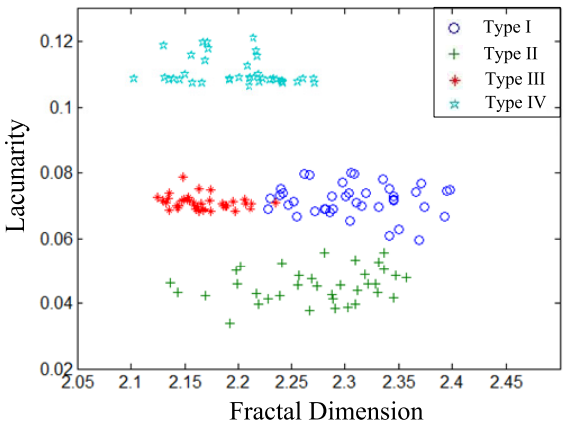


**FIGURE 14.** Distribution of HHT-derived characteristics of four defects.

**Step 2**: Extract the PD features (i.e., the fractal dimension and lacunarity).

**Step 3**: Calculate the degree of the correlation.

$$K(x) = \begin{cases} \dfrac{-2\rho(x, X_0)}{b - a}, & x \in X_o \\ \dfrac{\rho(x, X_0)}{\rho(x, X) - \rho(x, X_0)} & x \notin X_0 \end{cases} \tag{6}$$

where

$$\rho(x, X_0) = \left| x - \frac{a + b}{2} \right| - \frac{b - a}{2} \tag{7}$$

$$\rho(x, X) = \left| x - \frac{f + g}{2} \right| - \frac{g - f}{2} \tag{8}$$

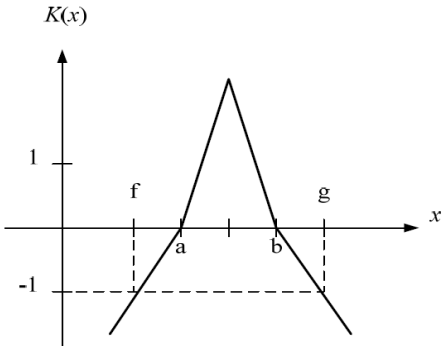


**FIGURE 15.** Extension membership function.

which relates the *j*th feature of the tested PD pattern to the *j*th input feature of the *i*th defect type as in Step 1.

**Step 4**: Set the weights of respective features $W_1$, $W_2$. In this study, the weights of all features were set to be equal.

**Step 5**: Evaluate the correlation index related to each defect type.

$$\zeta_i = \sum_{j=1}^{2} W_j K_{ij} \tag{9}$$

**Step 6**: Normalize the correlation index.

$$\lambda_i = \frac{2\zeta_i - \zeta_{\min} - \zeta_{\max}}{\zeta_{\max} - \zeta_{\min}} \tag{10}$$

which falls between $[-1, 1]$ and is seen as a significant quantity for pattern recognition.

**TABLE 1.** Cs clustering result: FD-Λ.

| Model \ Noise | 0% | ±10% | ±20% | ±30% |
|---|---|---|---|---|
| Type I | 100 | 90 | 85 | 65 |
| Type II | 100 | 70 | 60 | 55 |
| Type III | 100 | 85 | 65 | 50 |
| Type IV | 100 | 100 | 100 | 85 |
| Average | 100 | 86.3 | 77.5 | 63.8 |

### C. RECOGNITION RESULT

The extension method was used to identify defects. The first 20 extracted data points were selected as the set of clustered data for training. The remaining 20 data points were used in the recognition test, thus yielding the results presented in Tables 1 and 2. Random uniformly distributed noise was generated on the basis of the PD signal. Under a condition of 0% noise, the proposed method could identify the four defect types with 100% accuracy; under a condition of 10% noise, the average recognition rate was 86.3%. However, the HHT method was determined to have an 83.8% recognition rate. The CS method had a higher recognition rate than did the HHT method under noisy conditions. The proposed method incorporates fractal dimension and lacunarity characteristics. The clustering result revealed a relatively high level of effectiveness. Incorporating a third characteristic into the proposed method may increase the recognition rate under noise conditions. These results demonstrate that the proposed method can effectively distinguish the four defect types and extract crucial characteristic information regarding the four defect types.

**TABLE 2.** HHT clustering result: FD-Λ.

| Model \ Noise | 0% | ±10% | ±20% | ±30% |
|---|---|---|---|---|
| Type I | 100 | 80 | 75 | 60 |
| Type II | 100 | 80 | 65 | 55 |
| Type III | 95 | 85 | 50 | 50 |
| Type IV | 100 | 90 | 90 | 70 |
| Average | 98.8 | 83.3 | 70 | 58.8 |

## V. CONCLUSION

The present study evaluated four cable types: a standard cable, one with a scratched insulation layer, one with an excessively short insulation layer, and one with an excessively long insulation layer. The PD characteristics of each cable type were measured through the application of the HFCT method. Analysis was performed using a master–slave system for the power cable models; the status of the power cable (i.e., the ''master'') was assessed by inspecting the dynamic trajectory of the error signal. Fractal theory was employed to extract the trajectory properties of fractal dimensionality and lacunarity related to the various cable types. Additionally, for the purpose of accomplishing automatic defect recognition, this study developed a clustering algorithm based on extension theory. This algorithm demonstrated a clustering performance level superior to that of the HHT method, thus proving that it offers more reliable defect detection during the installation or fabrication of power cable systems in the service stage.

## REFERENCES

[1] Z. Guozhi, X. Zhang, H. Xingrong, Y. Jia, J. Tang, Z. Yue, T. Yuan, and L. Zhenze, ''On-line monitoring of partial discharge of less-oil immersed electric equipment based on pressure and UHF,'' *IEEE Access*, vol. 7, pp. 11178–11186, 2019.

[2] X. Chen, Y. Qian, Y. Xu, G. Sheng, and X. Jiang, ''Energy estimation of partial discharge pulse signals based on noise parameters,'' *IEEE Access*, vol. 4, pp. 10270–10279, 2016.

[3] C. Mazzetti, F. M. F. Mascioli, F. Baldini, M. Panella, R. Risica, and R. Bartnikas, ''Partial discharge pattern recognition by neuro-fuzzy networks in heat-shrinkable joints and terminations of XLPE insulated distribution cables,'' *IEEE Trans. Power Del.*, vol. 21, no. 3, pp. 1035–1044, Jul. 2006.

[4] H. Ma, J. C. Chan, T. K. Saha, and C. Ekanayake, ''Pattern recognition techniques and their applications for automatic classification of artificial partial discharge sources,'' *IEEE Trans. Dielectr. Electr. Insul.*, vol. 20, no. 2, pp. 468–478, Apr. 2013.

[5] F. Zeng, S. Wu, X. Yang, Z. Wan, J. Tang, M. Zhang, and Q. Yao, ''Fault diagnosis and condition division criterion of DC gas insulating equipment based on $SF_6$ partial discharge decomposition characteristics,'' *IEEE Access*, vol. 7, pp. 29869–29881, 2019.

[6] F. Petzold, H. Schlapp, E. Gulski, P. P. Seitz, and B. Quak, "Advanced solution for on-site diagnosis of distribution power cables," *IEEE Trans. Dielectrics Electr. Insul.*, vol. 15, no. 6, pp. 1584–1589, Dec. 2008.
[7] M. Wu, H. Cao, J. Cao, H. L. Nguyen, J. B. Gomes, and S. P. Krishnaswamy, "An overview of state-of-the-art partial discharge analysis techniques for condition monitoring," *IEEE Elect. Insul. Mag.*, vol. 31, no. 6, pp. 22–35, Nov./Dec. 2015.
[8] A. Bouzida, O. Touhami, R. Ibtiouen, A. Belouchrani, M. Fadel, and A. Rezzoug, "Fault diagnosis in industrial induction machines through discrete wavelet transform," *IEEE Trans. Ind. Electron.*, vol. 58, no. 9, pp. 4385–4395, Sep. 2011.
[9] S. M. Gargari, P. A. A. F. Wouters, P. C. J. M. van der Wielen, and E. F. Steennis, "Partial discharge parameters to evaluate the insulation condition of on-line located defects in medium voltage cable networks," *IEEE Trans. Dielectr. Electr. Insul.*, vol. 18, no. 3, pp. 868–877, Jun. 2011.
[10] W. Huang, Z. Shen, Y. C. Fung, and N. E. Huang, "Use of intrinsic modes in biology: Examples of indicial response of pulmonary blood pressure to ± step hypoxia," *Proc. Nat. Acad. Sci. USA*, vol. 95, no. 22, pp. 12766–12771, Oct. 1998.
[11] A. G. Espinosa, J. A. Rosero, J. Cusidó, L. Romeral, and J. A. Ortega, "Fault detection by means of Hilbert–Huang transform of the stator current in a PMSM with demagnetization," *IEEE Trans. Energy Convers.*, vol. 25, no. 2, pp. 312–318, Jun. 2010.
[12] E. Gulski, "Digital analysis of partial discharges," *IEEE Trans. Dielectr. Electr. Insul.*, vol. 2, no. 5, pp. 822–837, Oct. 1995.
[13] X. Zeng, Y. Xu, and Y. Wang, "Some novel techniques for insulation parameters measurement and Petersen-coil control in distribution systems," *IEEE Trans. Ind. Electron.*, vol. 57, no. 4, pp. 1445–1451, Apr. 2010.
[14] H.-T. Yau, C.-L. Kuo, and J.-J. Yan, "Fuzzy sliding mode control for a class of chaos synchronization with uncertainties," *Int. J. Nonlinear Sci. Numer. Simul.*, vol. 7, no. 3, pp. 333–338, 2006.
[15] C.-H. Huang, C.-H. Lin, and C.-L. Kuo, "Chaos synchronization-based detector for power-quality disturbances classification in a power system," *IEEE Trans. Power Del.*, vol. 26, no. 2, pp. 944–953, Apr. 2011.
[16] H.-C. Chen, H.-T. Yau, and P.-Y. Chen, "Chaos synchronization error technique-based defect pattern recognition for GIS through partial discharge signal analysis," *Entropy*, vol. 16, no. 8, pp. 4566–4582, Aug. 2014.
[17] K. A. Loparo, M. L. Adams, W. Lin, M. F. Abdel-Magied, and N. Afshari, "Fault detection and diagnosis of rotating machinery," *IEEE Trans. Ind. Electron.*, vol. 47, no. 5, pp. 1005–1014, Oct. 2000.
[18] W. I. Friesen and R. J. Mikula, "Fractal dimensions of coal particles," *J. Colloid Int. Sci.*, vol. 120, no. 1, pp. 263–271, Nov. 1987.
[19] F.-C. Gu, H.-C. Chang, and C.-C. Kuo, "Gas-insulated switchgear PD signal analysis based on Hilbert-Huang transform with fractal parameters enhancement," *IEEE Trans. Dielectr. Electr. Insul.*, vol. 20, no. 4, pp. 1049–1055, Aug. 2013.
[20] W. Liu and G. Chen, "A new chaotic system and its generation," *Int. J. Bifurcation Chaos*, vol. 13, no. 1, pp. 261–268, Feb. 2003.
[21] R. J. Jackson, A. Wilson, and D. B. Giesner, "Partial discharges in power-cable joints: Their propagation along a crossbonded circuit and methods for their detection," *IEE Proc. C-Gener., Transmiss. Distrib.*, vol. 127, no. 6, pp. 420–429, Nov. 1980.
[22] *Power Cables With Extruded Insulation and Their Accessories for Rated Voltages From 1 kV ($U_m$ = 1,2 kV) up to 30 kV ($U_m$ = 36 kV)—Part 2: Cables for Rated Voltages From 6 kV ($U_m$ = 7,2 kV) up to 30 kV ($U_m$ = 36 kV)*, Standard IEC 60502-2, 1998.
[23] F. Gu, H. Chen, and M. Chao, "Application of improved Hilbert–Huang transform to partial discharge defect model recognition of power cables," *Appl. Sci.*, vol. 7, no. 10, p. 1021, Oct. 2017.
[24] W. Cai, "The extension set and incompatibility problem," *J. Sci. Explor.*, vol. 1, no. 1, pp. 81–93, 1983.
[25] M.-H. Wang and C.-Y. Ho, "Application of extension theory to PD pattern recognition in high-voltage current transformers," *IEEE Trans. Power Del.*, vol. 20, no. 3, pp. 1939–1946, Jul. 2005.

**FENG-CHANG GU** was born in Taichung, Taiwan, in 1985. He received the B.S. and M.S. degrees from the National Chin-Yi University of Technology, Taichung, in 2007 and 2009, respectively, and the Ph.D. degree from the National Taiwan University of Science and Technology, in 2013. In 2018, he joined the National Chin-Yi University of Technology. His research interests include partial discharge detection, fault diagnosis, and pattern recognition.

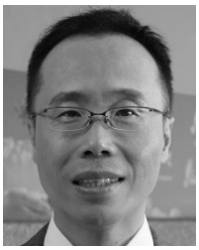

**HER-TERNG YAU** received the B.S. degree from National Chung Hsing University, Taichung, Taiwan, in 1994, and the M.S. and Ph.D. degrees from National Cheng Kung University, Tainan, Taiwan, in 1996 and 2000, respectively, all in mechanical engineering. He is currently a Professor with the Department of Electrical Engineering, National Chin-Yi University of Technology, Taichung. He has authored more than 150 research articles on a wide variety of topics in mechanical and electrical engineering. His research interests include energy converter control, system control of mechatronics, and nonlinear system analysis and control.

**HUNG-CHENG CHEN** was born in Chiayi, Taiwan, in 1965. He received the M.S. and Ph.D. degrees in electrical engineering from the National Taiwan University of Science and Technology, in 1989 and 1993, respectively. In 1993, he joined the National Chin-Yi University of Technology, Taichung, Taiwan, as a Faculty Member, where he is currently a Professor with the Department of Electrical Engineering. His research interests include fault diagnosis, partial discharge, micro-grid, and smart grid.